THE ASTROPHYSICAL JOURNAL, 485:409–418, 1997 August 10

INTENSITY AND DIRECTIONALITY OF FLARE-ACCELERATED α-PARTICLES AT THE SUN

GERALD H. SHARE AND RONALD J. MURPHY
E. O. Hulburt Center for Space Research, Naval Research Laboratory, Washington, DC 20375
Received 1996 October 29; accepted 1997 March 11

ABSTRACT

We have studied γ-ray line emission from fusion of accelerated α-particles with ambient helium in 19 solar flares observed by the *Solar Maximum Mission* Gamma-Ray Spectrometer from 1980 to 1989. An isotropic or fan-beam distribution of accelerated particles provides good fits to the line profiles for most of the flares. In contrast, a downward beam of accelerated particles can be ruled out at high confidence levels, 99.99% and 99.8%, for the two most intense flares and provides significantly poorer fits than isotropic or fan-beam distributions in two other flares. The fluences in the α-α lines, with a few exceptions, show a correlation with fluences of the narrow nuclear de-excitation lines from elements with high first ionization potential. If we assume that all accelerated ions have the same spectral shape, and if we adopt accelerated particle and ambient abundances derived from other γ-ray line studies, we find that an accelerated α/proton ratio of 0.5 is consistent with the spectra from the 19 flares, whereas a ratio of 0.1 is not. We also suggest the possibility that ^{7}Be produced in α-^{4}He fusion during the intense flares occurring in late 1989 may have reached Earth in a concentration high enough to account, in part, for ^{7}Be observed in NASA's *Long-Duration Exposure Facility* satellite after its recovery in early 1990.

Subject headings: nuclear reactions, nucleosynthesis, abundances — Sun: flares — Sun: particle emission — Sun: X-rays, gamma rays

1. INTRODUCTION

The angular distribution of energetic particles interacting in the corona and chromosphere reflects their acceleration and transport. Kozlovsky & Ramaty (1977) have shown that the shapes of γ-ray lines at 0.429 and 0.478 MeV can be used to infer the angular distributions of flare-accelerated α-particles. These lines result from de-excitation of ^{7}Be and ^{7}Li produced in fusion of the accelerated α-particles with ambient ^{4}He (Kozlovsky & Ramaty 1974). Murphy, Kozlovsky, & Ramaty (1988) have calculated the expected shapes of these lines for four different angular distributions of particles: isotropic, fan beam, broadened fan beam, and downward beam. They presented line profiles for flares at Sun center and at the limb.

Murphy et al. (1990) continued this study using a magnetic loop model for transport of the ions, including the effects of mirroring and MHD pitch-angle scattering. They also folded their calculations through the instrument response of the *Solar Maximum Mission* (*SMM*) Gamma-Ray Spectrometer (GRS) and compared the results with spectra observed from the 1981 April 27 solar flare. These comparisons provided convincing evidence for the presence of the α-α fusion lines in that flare. They showed that the quality of data was good enough to distinguish limb flares (as this one was) from disk-centered flares. Their fits also suggested that a downward beam of particles did not fit the data as well as an isotropic or fan-beam geometry.

In principle, the accelerated α-particle/proton ratio can be obtained by comparing the fluences of the α-α and narrow nuclear de-excitation lines. Determining the α/proton ratio is dependent on knowing the relative abundances of ambient He and the elements producing the narrow lines in the interaction region as well as the accelerated particle spectrum. Unfortunately, direct measurements of the solar He abundances are uncertain. Photospheric He cannot be measured directly but is inferred from stellar evolution models, yielding an He/H ratio of 0.095 (Grevesse, Noels, & Sauval 1996). Laming & Feldman (1994) used a UV spectrum over a sunspot to obtain an He/H ratio in the range of 0.078 to 0.22. A more precise abundance ratio, 0.07 ± 0.011, for the solar corona was reported by Gabriel et al. (1995). Long-term measurements of the solar wind typically give smaller He/H ratios, 0.03–0.05; however, the ratio can be highly variable on short timescales, ranging from 0.001 to over 0.3 (Gloeckler & Geiss 1989).

The intensity of the α-α line feature measured by Murphy et al. (1990) suggested that the accelerated α-particle fluence, the ambient ^{4}He abundance, or both are enhanced over accepted solar abundances. Murphy et al. (1991) evaluated accelerated-particle and ambient-gas abundances from the *SMM* γ-ray spectrum of the 1981 April 27 flare. Their analysis included detailed cross sections for all the critical reactions. They found the best fits to the data for different assumptions concerning the composition of the ambient material and the composition and spectra of the accelerated particles. They found that the α/proton ratio was higher than one would have anticipated from measurements of solar energetic particles in space. The best fits gave α/proton ratios ranging from 0.5 to 1, under the assumption that their spectral shapes were the same and that the ambient He/H ratio was 0.1. Some poorer fits yielded ratios closer to 0.3, however. This compares with ratios ranging from as small as $\sim$0.005 to as high as $\sim$0.3 for 4.4–6.4 MeV nucleon^{-1} particles observed in impulsive solar energetic particle events (Reames, Meyer, & von Rosenvinge 1994); this range in particle energies lies just below the threshold of the α-α fusion process. It is therefore important to determine whether the apparently high α/proton ratio measured for the 1981 April 27 flare is characteristic of all 19 flares observed by *SMM* and whether the ratios have as large a dispersion as those measured for the solar energetic particles.

In this paper we expand the study of the α-α fusion lines

TABLE 1

PARAMETERS OF 19 FLARES USED IN THIS STUDY

Flare	Date	Angle (deg)	Accumulation (s)	Probability (%)	α-α Lines (γ cm^{-2})	Narrow γ Lines[a] (γ cm^{-2})
1	1981 Apr 10	38	376[b]	13	4.3 ± 4.5	18.2 ± 2.5
			524	2	5.9 ± 4.9	23.5 ± 3.1
2	1981 Apr 27	91	1441[b]	35	21.8 ± 9.1	73.3 ± 5.3
			1916	9	37.8 ± 10.2	113.1 ± 6.2
3	1982 Jun 3	72	1195	23	−6.3 ± 9.2	28.6 ± 6.9
4	1982 Jul 9	73	245[b]	38	7.4 ± 5.7	23.6 ± 2.9
			327	0.5	18.6 ± 7.0	33.6 ± 3.4
5	1982 Nov 26	87	393	25	8.2 ± 5.2	16.2 ± 2.7
6	1982 Dec 7	80	1048[b]	29	−4.1 ± 10.2	54.3 ± 4.6
			2703	<0.1	−14.6 ± 17.2	147.9 ± 8.8
7	1984 Apr 24	45	925[b]	13	−5.1 ± 8.6	45.1 ± 5.7
			1097	2	−7.7 ± 8.6	55.3 ± 6.2
8	1986 Feb 6	2	1228	90	0.5 ± 7.6	45.4 ± 4.5
9	1988 Dec 16	43	2293[b]	15	61.7 ± 13.5	133.3 ± 7.6
			3555	1	101.6 ± 15.6	219.6 ± 10.7
10	1989 Mar 6	76	1376[b]	3.8	32.3 ± 11.0	77.5 ± 5.1
			3515	<0.1	80.9 ± 20.3	293.8 ± 11.6
11	1989 Mar 10	44	1834[b]	16	18.4 ± 10.4	61.3 ± 5.2
			3341	<0.1	27.8 ± 12.8	108.5 ± 7.5
12	1989 Mar 17	70	835	19	13.5 ± 8.4	48.8 ± 4.6
13	1989 May 3	44	1376	55	12.4 ± 6.5	24.3 ± 4.1
14	1989 Aug 16	87	916	79	23.4 ± 6.5	45.9 ± 3.9
15	1989 Aug 17	90	2228	23	13.3 ± 13.8	54.4 ± 7.3
16	1989 Sep 9	30	541	87	5.2 ± 5.4	17.0 ± 2.9
17	1989 Oct 19	32	3260	25	80.9 ± 12.6	179.7 ± 10.3
18	1989 Oct 24	64	573[b]	4.4	8.9 ± 8.5	42.1 ± 4.8
			819	0.3	12.9 ± 8.2	44.7 ± 3.7
19	1989 Nov 15	30	1048[c]	2.5	14.3 ± 7.8	35.7 ± 4.3
			1016	1.5	18.3 ± 7.2	32.6 ± 4.4

[a] Resolved nuclear de-excitation lines (Share & Murphy 1995).
[b] Corrected data.
[c] Different accumulation and background subtraction used.

to a sample of 19 solar flares observed by the *SMM* GRS with significant nuclear line emission (Share & Murphy 1995). In Share & Murphy (1995) the full 0.3–8.5 MeV spectra were used to obtain both the fluences and ratios of the nuclear de-excitation lines in the flares. In the current analysis, we fitted spectral data in the 0.3–0.75 MeV energy range with an incident photon spectrum comprising five individual components, including the α-α line feature; this contrasts with the work of Murphy et al. (1991), in which the parameters of the accelerated particles producing the γ-rays were varied. In the next section we discuss how the data were accumulated and the fits that were performed. In § 3 we discuss the results of our fits as they relate to both the inferred directionality of the accelerated α-particles and the accelerated α/proton ratio. We discuss the implications of these observations in § 4.

2. SPECTROSCOPIC STUDIES OF THE α-α LINES IN *SMM* DATA

Time-integrated spectra from 0.3 to 8.5 MeV have been accumulated for 19 flares with significant emission of narrow de-excitation lines (Share & Murphy 1995). The accumulations were made for all times, excluding intervals during which the instrument was saturated or telemetry errors occurred. In that earlier study, the full energy range was fitted with a photon model containing a bremsstrahlung continuum and 18 narrow- and broad-line features. In this study we concentrate on the energy range from 0.3 to 0.75 MeV in order to improve sensitivity to the α-α fusion lines.

In this limited energy range, we use an incident photon model containing a bremsstrahlung function, a narrow 511 keV annihilation line, a positronium continuum, instrumentally degraded radiation from nuclear lines above 0.75 MeV, and various line shapes for the fusion lines. We use a simple power law in energy to represent the bremsstrahlung continuum and obtain its amplitude and exponent. For this study we have fixed the annihilation line energy and set its width at a nominal 10 keV; the amplitude of the line is a free parameter. The amplitude of the positronium continuum is also a free parameter but is constrained to be positive. The amplitude of the degraded nuclear component reflects the nuclear de-excitation and 2.223 MeV line fluxes. In this study we have allowed the amplitude to be a free parameter to take into account inaccuracies in the instrument response function as well as any scattered radiation from the Sun; with the exception of two or three flares (see later discussion), the implied fluxes of higher energy emission from our fits to the 0.3–0.75 MeV data agree well with those determined by Share & Murphy (1995) over the higher energy range. Whether this scattered nuclear component was free or fixed had no significant impact on the α-α line fluxes, however.

The α-α line profiles for three basic particle geometries—isotropic, fan beam, and downward beam—have been determined for the heliocentric angle of each flare. These normalized line profiles (Murphy et al. 1988; R. Ramaty, B. Kozlovsky, R. E. Lingenfelter, & R. J. Murphy 1996, private communication) were multiplied by a free parameter that is determined by the fit. The fan-beam geometry approximates the distribution expected for particles experiencing no pitch-angle scattering, while the downward beam approximates the distribution for particles experiencing strong pitch-angle scattering (Murphy et al. 1990). We shall later use the results of these fits to determine which accelerated particle geometry is preferred.

The composite model, with initial estimates of the free parameters, is folded through a matrix representing the instrument response function and compared with the observed count spectrum. The values of the parameters are then sequentially varied with a computer algorithm until the χ^2 parameter is minimized. Not all of these fits gave acceptable values of χ^2; this is reflected in the low probability that the data are statistically distributed about the model. The poor fits were in large part due to specific time intervals in the flares during which telemetry errors occurred or the rates were high enough that the instrument model was not adequate. For purposes of studying α-particle directionality, we adopted a criterion that the original fits be acceptable at the 10% level. For those flares that had lower probabilities, we fitted individual 1 minute accumulations and removed those for which the fits were unacceptable; we then produced a corrected integrated spectrum for the flare.

The results of the fits for the 19 flares are summarized in Table 1. Listed are the time over which the spectral accumulations were made, the percentage of fits of randomly distributed data with higher values of χ^2, and the fluence in the α-α lines for the isotropic model. Where two entries are provided in the table for a specific flare, the top one is for the corrected spectrum and the bottom one is for the original spectrum. For comparison, we also list the fluence in the narrow nuclear de-excitation lines derived from fits to the full 0.3–8.5 MeV energy range (Share & Murphy 1995). For some flares, additional data selections were required to achieve reasonable fits. For two flares, on 1982 December 7 and 1989 March 6, we also removed 1 minute accumulations with high electron bremsstrahlung to nuclear line ratios from the corrected spectra. For the flare on 1988 December 16, we deleted the lowest energy channel, and for the flare on 1989 March 10, we fitted the spectrum only up to 0.7 MeV because of systematic errors in the data. We also marginally improved the fit to the 1989 November 15 spectrum by using an improved background subtraction technique developed for searching for short celestial transients (Share et al. 1993). We have studied whether there are any statistically significant changes in the α-α/narrow nuclear line ratios in comparing the original and corrected spectra and have not found any. Overall, we improved the acceptability of the fits significantly; however, there still are three flares for which the acceptability did not exceed the desired 10%.

3. RESULTS

3.1. *Directionality of Accelerated α-Particles*

In this section we compare the results of our fits for accelerated α-particles having isotropic, fan-beam, and downward-beam geometries. The fan-beam and isotropic distributions are not readily distinguishable from one another with an instrument, such as the GRS, with moderate spectral resolution. This is true even for flares located near the center of the solar disk, where the lines produced by a fan beam appear at their rest energies and are not broadened significantly (see Fig. 2 of Murphy et al. 1988). We use these simple geometric distributions because the line profiles are easily calculable at all the heliocentric angles. Future comparisons will incorporate a physical model of particle transport similar to that used by Murphy et al. (1990).

Plotted in Figure 1 are the corrected spectra for the 19 flares. The best-fit components for each flare are plotted separately for two particle geometries: isotropic (*left-hand panels*) and a downward-directed beam (*right-hand panels*). The α-α line profiles for the downward-beam geometry are dependent on heliocentric angle. For clarity we have subtracted the best-fit bremsstrahlung function from the spectral data before plotting; for this reason, the spectra in the right- and left-hand panels differ from one another. The change in the downward-beam line profile with heliocentric angle is most evident when comparing the right-hand panels for the 1981 April 27 and 1986 February 6 flares. The fusion lines are at their rest energies for the April limb event but are redshifted for the disk-centered event in February. The 511 keV line and associated positronium continuum show flare-to-flare variability; this variation is the subject of another paper.

The overall goodness of the fit, the percentage of fits to randomly distributed data that would give higher values of the χ^2 statistic, is shown for both particle geometries for each flare (note that we have used the corrected spectra for this analysis; see Table 1). Table 2 summarizes these probabilities for all three geometries: isotropic, fan beam, and downward beam. There is no significant difference between the fits in the isotropic and fan-beam geometries, as is expected from our earlier discussion.

There is expected to be a significant difference between the α-α line shapes of isotropic and downward-beam geometries for flares near the disk center. There were nine flares that occurred at heliocentric angles of 45° or less. Four of these flares had isotropic α-α line fluxes significant at greater than 1.5 σ. The two flares in this sample with the most intense α-α lines show significant differences between fits for the two geometries. The isotropic/fan-beam geometry provides significantly better fits than does the downward-beam geometry. The 1988 December 16 flare occurred at a heliocentric angle of 43°; it is well fitted (15% probability) by the isotropic geometry, but the shifted profile of the downward-beam geometry provides a poor fit to the data (0.2% probability). The 1989 October 19 flare at a heliocentric angle of 32° shows an even greater disparity between the quality of fits for the isotropic/fan-beam geometries (25% probability) and downward-beam geometry (0.01% probability). For the two weaker flares on 1989 March 10 and November 15, the isotropic/fan-beam geometry is also marginally preferred. All three particle distributions gave acceptable fits for the 1981 April 27 flare with the reduced data set; this contrasts with the earlier result of Murphy et al. (1990) that suggested that an isotropic particle distribution fitted the data better than a downward beam for this limb event.

We conclude from this analysis that a downward-beam geometry for the accelerated α-particles is inconsistent with our fits to the spectra with the most significant α-α lines.

3.2. *Accelerated α/Proton Ratio*

As discussed in § 1, a measure of the accelerated α/proton ratio can be obtained by comparing the fluences of the α-α

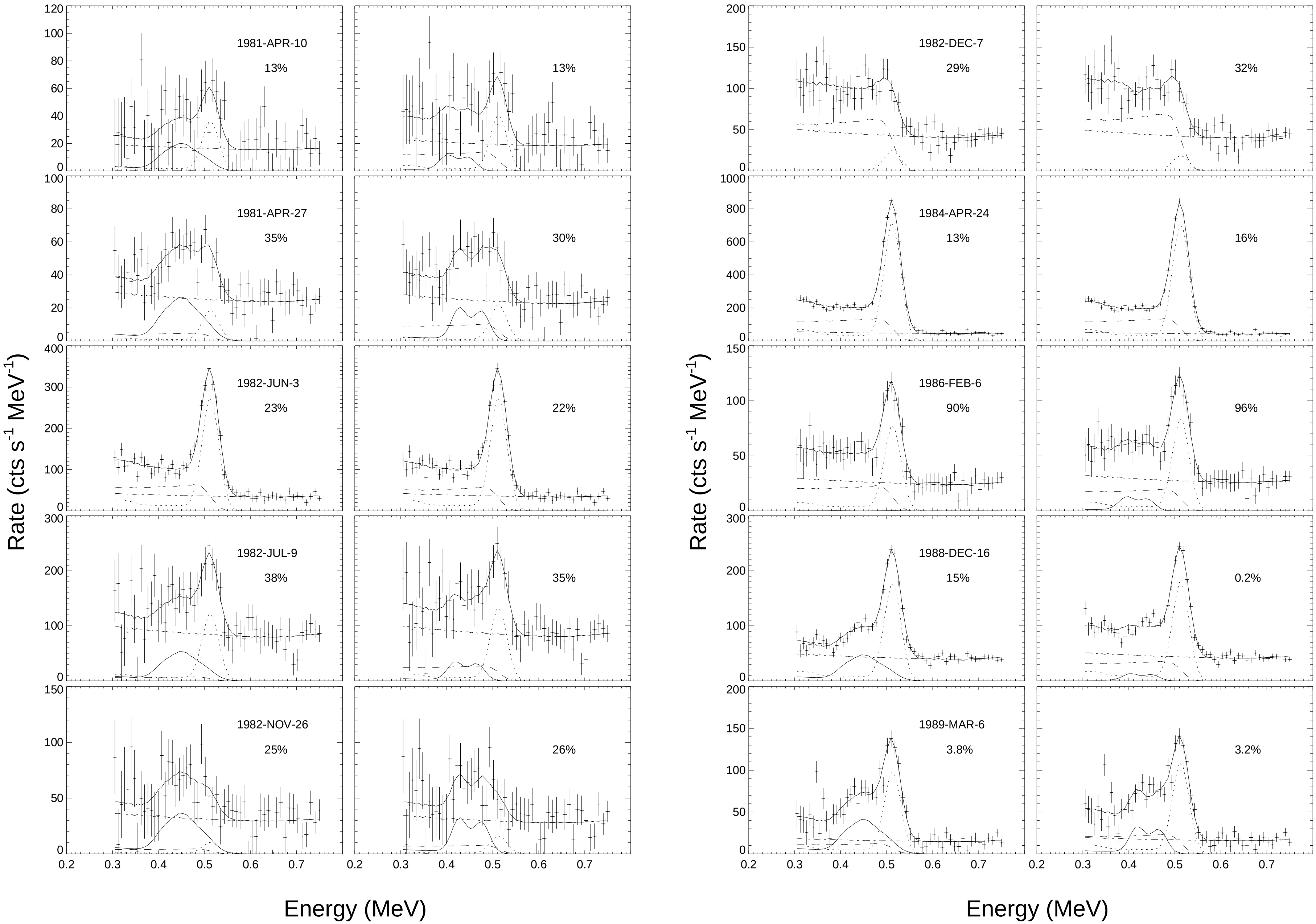

FIG. 1.—*SMM* GRS spectra of flares from 0.3 to 0.75 MeV that have strong emission of nuclear lines. The fitted bremsstrahlung component has been subtracted. The plotted errors are statistical. Best-fitting components: *light solid curve*, α-α lines; *dotted curve*, 511 keV annihilation line; *dashed curve*, 3 γ continuum from positronium formation; *dot-dashed curve*, nuclear component; *heavy solid curve*, total fit. *Left-hand panels:* isotropically distributed α-particles; *right-hand panels:* α-particles in a downward-beam geometry.

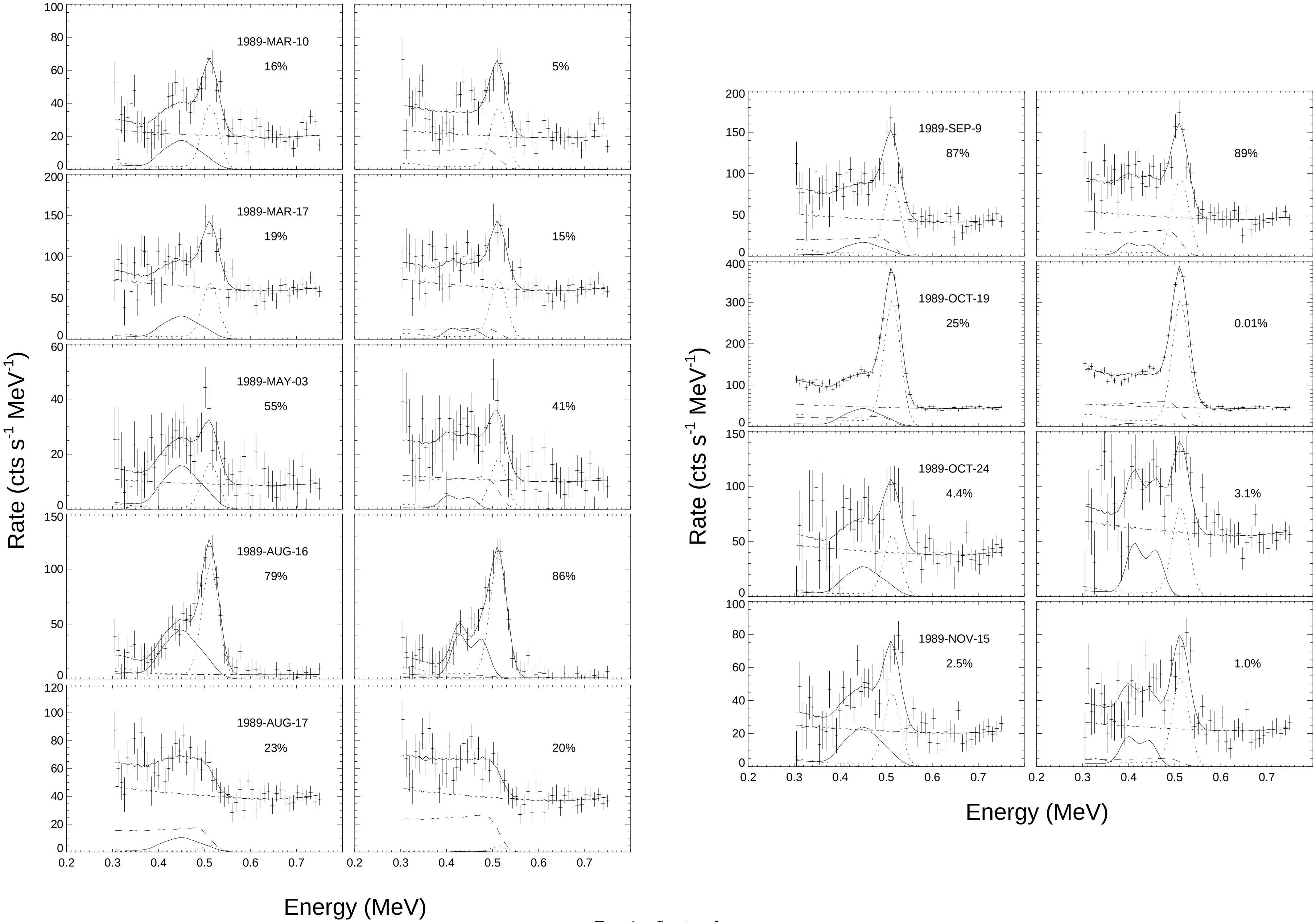

FIG. 1—*Continued*

TABLE 2

DIRECTIVITY STUDY

Flare	Date	Angle (deg)	Probability of Good Fit (%) Isotropic	Fan Beam	Downward Beam
1.......	1981 Apr 10	38	13	14	13
2.......	1981 Apr 27	91	35	32	30
3.......	1982 Jun 3	72	23	23	22
4.......	1982 Jul 9	73	38	38	35
5.......	1982 Nov 26	87	25	23	26
6.......	1982 Dec 7	80	29	28	32
7.......	1984 Apr 24	45	13	13	16
8.......	1986 Feb 6	2	90	91	96
9.......	1988 Dec 16	43	15	21	0.2
10......	1989 Mar 6	76	3.8	3.5	3.2
11......	1989 Mar 10	44	16	16	5
12......	1989 Mar 17	70	19	20	15
13......	1989 May 3	44	55	57	41
14......	1989 Aug 16	87	79	73	86
15......	1989 Aug 17	90	23	23	20
16......	1989 Sep 9	30	87	86	89
17......	1989 Oct 19	32	25	28	0.01
18......	1989 Oct 24	64	4.4	3.9	3.1
19......	1989 Nov 15	30	2.5	1.5	1.0

and narrow nuclear de-excitation lines. As He has a high first ionization potential (FIP = 24.6 eV), it is best to use de-excitation lines only from elements with high FIPs, such as C, O, N, and Ne, in making these comparisons. This is true because Share & Murphy (1995) showed that the low-FIP/high-FIP line ratio is variable from flare to flare. Table 3 lists the α-α line fluences derived from the preferred isotropic model (see above) and fluences of the high-FIP de-excitation lines at 1.63 MeV (Ne), 4.43 MeV (C, O [spallation]), 6.13 MeV (O), and $\sim$6.9 MeV (O) integrated over the entire flare; it also lists the sum of the four high-FIP lines. We use spectra integrated over the entire flare in this section in order to be compatible with earlier studies (e.g., Share & Murphy 1995; Ramaty, Mandzhavidze, & Kozlovsky 1996).

In Figure 2, the α-α line fluences are plotted against the sum of the fluences in these four de-excitation lines. These two sets of fluences show a good correlation, with the exception of a few flares, for which the observed yields of the α-α lines are below the average. Plotted through the data is the best fit assuming a linear relationship between the fluences. The overall probability that the data come from a random sample distributed about the plotted slope is only 0.4% on the basis of the χ^2 statistic. The flare on 1982 December 7 is the primary reason for this large dispersion. Removing this flare from the sample improves the probability to 11%. The γ-ray spectrum from this flare (see Fig. 1) is unusual in that the 511 keV line is small relative to what appears to be the positronium continuum. Another flare that has these characteristics occurred on 1989 August 17. Both flares occurred at large heliocentric angles, 80° or greater. There is some evidence that scattering at the Sun may play a role in attenuation of the 511 keV line, and therefore the α-α lines, in these flares. For these flares, the fitted nuclear component over the 0.3–0.75 MeV range is higher than what we would have estimated using the higher energy line fluences derived

TABLE 3

LINE FLUENCES FOR 19 FLARES

Flare	α-α Lines (γ cm^{-2})	1.63 MeV (γ cm^{-2})	4.43 MeV (γ cm^{-2})	6.13 MeV (γ cm^{-2})	6.9 MeV (γ cm^{-2})	High FIP[a] (γ cm^{-2})
1.......	5.9 ± 4.9	6.5 ± 1.1	2.2 ± 0.8	3.2 ± 0.5	1.1 ± 0.5	13.0 ± 1.5
2.......	37.8 ± 10.2	19.5 ± 2.4	18.8 ± 1.9	14.5 ± 1.1	11.6 ± 1.1	64.6 ± 3.4
3.......	−6.3 ± 9.2	8.1 ± 2.4	9.5 ± 1.5	2.2 ± 0.8	1.7 ± 0.8	21.6 ± 3.0
4.......	18.6 ± 7.0	5.7 ± 1.2	5.1 ± 1.0	4.5 ± 0.6	2.4 ± 0.5	17.7 ± 1.7
5.......	8.2 ± 5.2	1.9 ± 1.0	1.1 ± 0.7	1.9 ± 0.4	2.3 ± 0.4	7.2 ± 1.4
6.......	−14.6 ± 17.2	35.3 ± 2.7	26.6 ± 2.2	21.7 ± 1.3	12.8 ± 1.2	96.5 ± 4.0
7.......	−7.7 ± 8.6	14.0 ± 2.0	11.9 ± 1.6	6.7 ± 1.0	3.2 ± 0.9	35.8 ± 2.9
8.......	0.5 ± 7.6	6.5 ± 1.7	6.5 ± 1.2	7.5 ± 0.7	3.4 ± 0.7	23.9 ± 2.3
9.......	101.6 ± 15.6	51.9 ± 3.3	46.5 ± 2.7	43.4 ± 1.7	22.8 ± 1.5	164.6 ± 4.8
10......	80.9 ± 20.3	64.2 ± 3.4	48.8 ± 2.9	39.8 ± 1.7	26.5 ± 1.6	179.2 ± 5.0
11......	27.8 ± 12.8	22.6 ± 2.7	14.0 ± 2.1	12.8 ± 1.3	7.9 ± 1.3	57.3 ± 3.9
12......	13.5 ± 8.4	9.4 ± 1.6	6.6 ± 1.3	7.1 ± 0.8	4.4 ± 0.7	27.5 ± 2.3
13......	12.4 ± 6.5	5.8 ± 1.6	3.3 ± 1.2	4.2 ± 0.7	2.4 ± 0.7	15.7 ± 2.2
14......	23.4 ± 6.5	11.7 ± 1.4	6.3 ± 1.3	6.5 ± 0.8	4.0 ± 0.8	28.6 ± 2.2
15......	13.3 ± 13.8	18.0 ± 2.6	11.6 ± 2.3	8.2 ± 1.4	3.3 ± 1.3	41.0 ± 4.0
16......	5.2 ± 5.4	1.9 ± 1.1	2.0 ± 0.9	3.8 ± 0.6	1.4 ± 0.5	9.1 ± 1.6
17......	80.9 ± 12.6	41.7 ± 2.9	36.1 ± 2.6	31.6 ± 1.6	15.4 ± 1.5	124.8 ± 4.4
18......	12.9 ± 8.2	10.0 ± 1.4	7.9 ± 1.2	8.4 ± 0.7	4.1 ± 0.7	30.5 ± 2.0
19......	18.3 ± 7.2	5.7 ± 1.5	6.5 ± 1.4	4.2 ± 0.8	3.1 ± 0.8	19.5 ± 2.3

[a] Sum of 1.63, 4.43, 6.13, and 6.9 MeV lines.

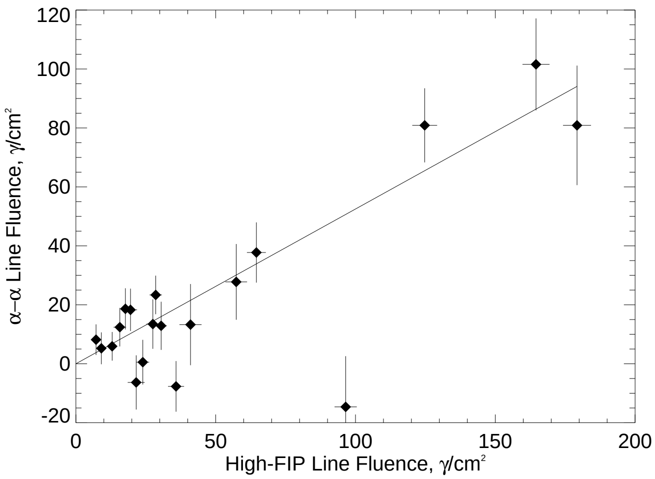

FIG. 2.—α-α line fluences, assuming isotropic α-particle angular distributions, plotted vs. the summed fluence in high-FIP lines at 1.63, 4.43, 6.13, and ∼6.9 MeV.

in our earlier analysis over the 0.3–8.5 MeV range (Share & Murphy 1995), which is suggestive of scattering of the photons at the Sun. We note, however, that the only other flare in the sample of 19 to exhibit the same difference in the scattered nuclear component was the one on 1989 March 17, at a heliocentric angle of 70°, but this event exhibited a relatively strong 511 keV line.

The correlation displayed in Figure 2 suggests that the α-α/high-FIP line ratios may be relatively constant from flare to flare. The observed ratios are listed in Table 4 and plotted in Figure 3*a*. This correlation also suggests that the accelerated α/proton ratio may also be relatively constant from flare to flare. The most accurate determination of the accelerated α/proton ratio in individual flares requires fits to the entire γ-ray spectrum while varying the spectra and composition of accelerated particles and the ambient abun-

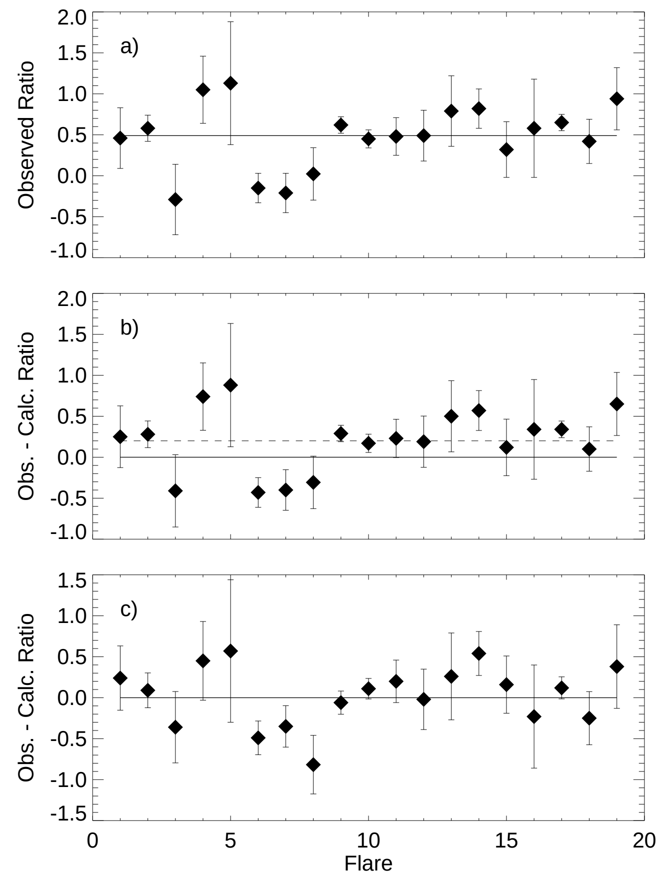

FIG. 3.—Comparison of observed and calculated α-α/high-FIP line ratios used to determine the accelerated α/proton ratio at the Sun. (*a*) Observed α-α/high-FIP line ratios; the solid line is the weighted mean. (*b*) Difference between observed and calculated line ratios for accelerated α/proton ratio of 0.1; the dashed line is the weighted mean and is significantly different from zero. (*c*) Same as (*b*), but for an α/proton ratio of 0.5; the weighted mean is consistent with zero.

TABLE 4

OBSERVED AND CALCULATED α-α/HIGH-FIP LINE RATIOS

		α-α/HIGH-FIP LINE RATIO		
			Calculated	
FLARE	DATE	Observed	α/proton = 0.1	α/proton = 0.5
1	1981 Apr 10	0.46 ± 0.38	0.21 ± 0.07	0.22 ± 0.13
2	1981 Apr 27	0.58 ± 0.16	0.30 ± 0.03	0.49 ± 0.14
3	1982 Jun 3	−0.29 ± 0.43	0.12 ± 0.10	0.07 ± 0.07
4	1982 Jul 9	1.05 ± 0.41	0.31 ± 0.03	0.60 ± 0.25
5	1982 Nov 26	1.13 ± 0.75	0.25 ± 0.06	0.56 ± 0.44
6	1982 Dec 7	−0.15 ± 0.18	0.28 ± 0.02	0.34 ± 0.10
7	1984 Apr 24	−0.21 ± 0.24	0.19 ± 0.06	0.14 ± 0.08
8	1986 Feb 6	0.02 ± 0.32	0.33 ± 0.01	0.84 ± 0.16
9	1988 Dec 16	0.62 ± 0.10	0.33 ± 0.01	0.68 ± 0.10
10......	1989 Mar 6	0.45 ± 0.11	0.28 ± 0.02	0.34 ± 0.06
11......	1989 Mar 10	0.48 ± 0.23	0.25 ± 0.04	0.28 ± 0.12
12......	1989 Mar 17	0.49 ± 0.31	0.30 ± 0.04	0.51 ± 0.20
13......	1989 May 3	0.79 ± 0.43	0.29 ± 0.06	0.53 ± 0.31
14......	1989 Aug 16	0.82 ± 0.24	0.25 ± 0.04	0.28 ± 0.12
15......	1989 Aug 17	0.32 ± 0.34	0.20 ± 0.06	0.16 ± 0.08
16......	1989 Sep 9	0.58 ± 0.60	0.24 ± 0.10	0.81 ± 0.19
17......	1989 Oct 19	0.65 ± 0.10	0.31 ± 0.02	0.53 ± 0.09
18......	1989 Oct 24	0.42 ± 0.27	0.32 ± 0.02	0.67 ± 0.18
19......	1989 Nov 15	0.94 ± 0.38	0.29 ± 0.06	0.56 ± 0.34

dances (Murphy et al. 1991). That analysis is beyond the scope of this paper. The approach we take here is to assume that the α/proton ratio is constant from flare to flare and to determine whether the relative yield in the α-α lines is consistent with the assumed ratio.

The yield in the α-α lines is dependent on the accelerated particle spectrum and ambient and accelerated particle composition. Ratios of γ-ray lines can be used to infer the spectra of accelerated particles. The ratio of the neutron capture line at 2.223 MeV to the carbon de-excitation line at 4.43 MeV has been used for several years. Because the 2.223 MeV line is delayed, it is important that the entire flare be observed. Spectral indices have been obtained from this ratio for nine *SMM* flares far from the solar limb, where limb darkening occurs for the 2.223 MeV line and for which we have complete data accumulations (see, e.g., Share & Murphy 1995; Ramaty et al. 1996). The ratio of the prompt de-excitation lines at 6.13 MeV and 1.63 MeV also provides an estimate of the spectral index of accelerated particles and can be used for all 19 flares (Share & Murphy 1995). Ramaty et al. (1996) found consistency between spectral indices derived with these two sets of line ratios under certain conditions: an accelerated particle spectrum following a power-law shape, particles impacting in a thick-target model with ambient elemental abundances adopted for the corona (Reames 1995) but with an elevated Ne/O ratio of 0.25, and impulsive flare composition for the acclerated particles with ^{3}He/^{4}He equal to 1 and α/proton ratios ranging from $\sim$0.1 to 0.5.

The dependence of the α-α/high-FIP line ratio on particle spectral index for α/proton ratios of 0.1 and 0.5 (R. Ramaty, B. Kozlovsky, R. E. Lingenfelter, & R. J. Murphy 1996, private communication) is plotted in Figure 4 for the conditions listed above. Steeply falling particle spectra do not readily produce the α-α lines. As the particle spectra harden to those with indices near -3, the production of the α-α lines increases because of the sharp rise in its cross section at $\sim$10 MeV; for even harder spectra, spallation reactions contribute significantly to the production of the de-excitation lines, causing the ratio to decrease.

Using Figure 4 and spectral indices derived from the graphical results provided in Figure 1 of Ramaty et al. (1996), we calculated the expected α-α/high-FIP line ratios for the 19 flares. These calculated line ratios and their 1 σ

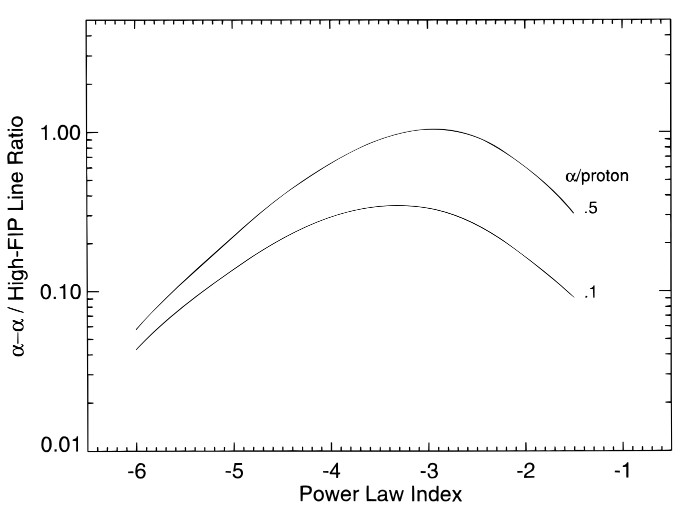

FIG. 4.—Calculated α-α/high-FIP line ratio plotted vs. the power-law spectral index for accelerated α/proton ratios of 0.1 and 0.5.

uncertainties are listed in Table 4 for accelerated α/proton ratios of 0.1 and 0.5. We plot the difference between the observed and calculated ratios for the 19 flares in Figures 3*b* and 3*c* for α/proton ratios of 0.1 and 0.5, respectively. The flare-to-flare spread in these differences is significantly decreased over the dispersion in the observed ratios. Probability that the spread is statistical increases to 2% for α/proton = 0.1 and to 17% for α/proton = 0.5 (this compares with 0.4% for the uncorrected ratios plotted in Fig. 1*a*). An α/proton ratio of 0.5 not only reduces the flare-to-flare variation to the statistical expectation but on average also predicts an α-α line yield closer to the observations. This is reflected in the weighted means of differences between the calculated and observed α-α/high-FIP ratios: for α/proton of 0.5, the mean, 0.01 ± 0.06, is consistent with zero; for α/proton of 0.1, the mean, 0.20 ± 0.046, is inconsistent with zero (probability 5×10^{-5}).

The relatively large errors in our measured line ratios prevent us from making a strong statement about the constancy of the accelerated α/proton ratio from flare to flare; however, we note that there is only one flare for which an α/proton ratio of 0.1 is a significant improvement over a ratio of 0.5. Our study suggests that the accelerated α/proton ratio is relatively constant from flare to flare and that its value is closer to 0.5 than to 0.1. We discuss the implications of this in the next section.

4. DISCUSSION AND SUMMARY

4.1. *Directionality of Accelerated α-Particles*

We have studied emission of the α-α fusion lines in 19 solar flares observed by the *Solar Maximum Mission* Gamma Ray Spectrometer from 1980 to 1989. The line profiles are dependent on both the accelerated particle directionality and the position of the flare on the Sun. Only the simple cases of isotropic, downward-beam, and fan-beam geometries have been studied here. Significant α-α line emission (>2 σ) was observed from eight of these flares. Four of these eight flares occurred at heliocentric angles smaller than 45°, where the downward-beam geometry can be distinguished from isotropic or fan-beam geometries. The isotropic/fan-beam geometries provide good fits to the α-α line profiles for the two flares emitting the highest fluences in this line; in contrast, the downward-beam geometry can be ruled out at high confidence levels, 99.99% and 99.8% for these flares. The downward-beam geometry also provides poorer fits to the line profiles than do the isotropic/fan-beam geometries in the other two strong flares at angles less than 45°. There is no significant difference in the quality of the fits of the line profiles for the remaining 15 flares. A fan-beam or isotropic distribution for accelerated particles was also found to be consistent with observations of neutrons from two flares (Hua & Lingenfelter 1987).

Physical models of particle transport in magnetic loops that take into account pitch-angle scattering have been derived by Murphy et al. (1990). A distribution with strong pitch-angle scattering is broader than the simple downward-beam function that we used here. On the basis of our experience with the downward beam, it may be possible to exclude a transport model with strong pitch-angle scattering by using *SMM* data for the two strong disk center flares.

Such strong pitch-angle scattering has been inferred from *Yohkoh* observations of γ-ray emission from a disk flare near its peak emission on 1991 November 15 (Yoshimori et al. 1994). We have some concerns about these observations and the authors' conclusions: (1) their fits are also consistent with an isotropic distribution; (2) the flare extended for at least 30 s, and yet only 4 s at the peak were used when the instrument suffered dead-time problems; and (3) the 4.4 MeV/α-α line ratio measured during this flare (Kotov et al. 1996) is more than an order of magnitude smaller than the mean value derived from the 19 *SMM* flares. We return to these concerns below.

4.2. *Accelerated α/Proton Ratio*

The fluences in the α-α fusion lines in 19 flares observed by *SMM* are generally correlated with fluences observed in the narrow nuclear de-excitation lines from proton and α-particle bombardment of high-FIP ambient elements. This suggests that the accelerated α/proton ratio is relatively constant from flare to flare. Determination of the α/proton ratio on a flare-to-flare basis requires fits to the entire γ-ray spectrum while varying the spectra and composition of accelerated particles and the ambient abundances (Murphy et al. 1991). As that analysis is beyond the scope of this paper, we studied whether the fluences in the α-α fusion lines are consistent with calculations for two α/proton ratios, 0.1 and 0.5. Ratios in this range have been found by Ramaty et al. (1996) to be consistent with other line measurements for these flares (Share & Murphy 1995) under the following conditions: (1) the accelerated particles have a composition representative of impulsive solar energetic particles and (2) the particles interact in a thick target with ambient elemental abundances adopted for the corona (Reames 1995), except that the He/H ratio is 0.1 and the Ne/O ratio is 0.25.

We find that the observed α-α line yields are consistent with calculations for an accelerated α/proton ratio of 0.5, and they are inconsistent (probability $<10^{-4}$) for a ratio of 0.1. This demonstrates that the high α/proton ratio found by Murphy et al. (1990) for the 1981 April 27 flare is generally characteristic of all 19 intense nuclear line flares observed by *SMM*. A recent observation of the 1991 June 4 flare by the Oriented Scintillation Spectrometer Experiment on the *Compton Gamma Ray Observatory* also measured an α/proton ratio consistent with a value of 0.5 and inconsistent with a value as low as 0.1 (Murphy et al. 1997).

Impulsive solar energetic particle data are available for only two of the 19 strong γ-ray line flares observed by *SMM*. Reames, Cane, & von Rosenvinge (1990) report an α/proton ratio of 0.016 ± 0.003 in the 1.9–2.8 MeV amu^{-1} energy interval from observations made by *ISEE 3* of the 1981 April 10 flare. Because the γ-ray yield from this flare was relatively small, we could not significantly constrain the accelerated α/proton ratio from our observations (see Fig. 3). No other impulsive particle events associated with the remaining 18 *SMM* flares were observed by *ISEE*. Solar energetic particles were well observed from the 1982 June 3 flare by detectors on *Helios 1* (Van Hollebeke, McDonald, & Meyer 1990). The α/proton ratio at $\sim$5 MeV amu^{-1} was $\sim$0.02 with a time of maximum analysis but appears much higher, $\sim$0.25, when the data are integrated over the entire event. Although we found no detectable α-α line emission from this flare, the data are still consistent with α/proton ratios of up to 0.5 because of the steep accelerated particle spectrum (power-law indices steeper than about -5) inferred from other line measurements (Ramaty et al. 1996). The solar energetic particle spectra measured by *Helios* in space are much harder, with indices ranging from about -2.3 to about -1.2. This spectral difference may be explained by the fact that this flare exhibited two distinct acceleration phases, with the second, less intense, more extended phase being considerably harder (Ramaty, Murphy, & Dermer 1987).

Our finding that the accelerated α/proton ratio inferred from the γ-ray measurements generally appears closer to 0.5 than to 0.1 contrasts with ratios derived from interplanetary particle measurements, which typically range from $\sim$0.005 to as high as $\sim$0.3. It is not clear whether the γ-ray flares represent a specific class of events with a high α/proton ratio or whether different acceleration processes produce particles impacting the Sun from those escaping the Sun. We must keep in mind, though, that the accelerated α/proton ratio inferred from the γ-ray measurements is dependent on other assumed parameters used in the calculations. If, for example, the ambient He/H ratio were larger than 0.1, the accelerated α/proton ratio would drop. Alternatively, current calculations assume that all the accelerated particles have the same spectral shape, a simple power law with the same spectral index for all particle species. Decoupling the proton and α-particle spectra could affect the value of the accelerated α/proton ratio derived from the γ-ray line measurements.

We do not know of any acceleration models that specifically predict high α/proton ratios in flare-accelerated particles interacting at the Sun. On the other hand, Miller & Reames (1996) discuss a model based on stochastic acceleration by cascading Alfvén wave turbulence that preferentially accelerates heavy ions with the lowest ion cyclotron frequency. These calculations yield heavy-ion ratios that are similar to those observed in solar energetic particles. Whether it can also account for an accelerated α/proton ratio of about 0.5 at the Sun needs to be determined.

4.3. *Implications for Be Observed in Earth Orbit and Li Abundances in Stars*

An extraordinarily high concentration of ^{7}Be at an altitude of 310 km has been inferred from measurements on samples of NASA's *LDEF* after its return to Earth in 1990 January (Fishman et al. 1991; Phillips et al. 1991). This radioactive isotope was observed primarily on the leading surfaces of *LDEF*, which suggests that it was swept up from the residual atmosphere. The absolute concentration of ^{7}Be needed to explain the observation is $\sim 10^{-7}$ atoms cm^{-3} at about 310 km. As pointed out by the authors, this is equivalent to a relative concentration of $\sim 4 \times 10^6$ atoms g^{-1} of air, which is $\sim$4000 times higher than what is measured between 20 and 50 km, where most of the ^{7}Be is believed to be produced by cosmic-ray spallation of nitrogen and oxygen.

Is it possible for some of this ^{7}Be to have its origin in the fusion of accelerated α-particles with He in flares that occurred in the 4 months preceding the recovery of *LDEF*? From Table 3 we note that the integrated fluence in the α-α lines observed at Earth is $\sim 110\ \gamma$ cm^{-2} for flares observed by *SMM* during this time. As 50% of this line flux comes as a result of the production of ^{7}Be but only 40% of the ^{7}Be nuclei yield a 429 keV γ-ray (Murphy et al. 1988), up to ~ 135 ^{7}Be atoms cm^{-2} could have reached Earth from these flares. This assumes that the ^{7}Be was emitted isotropically, similar to the γ-rays, and absorbed in the atmosphere with an efficiency of 100%; it does not take into account flares that may have been missed by *SMM*. Taking into account decay during the approximately two radioactive half-lives between the flares and the recovery of *LDEF* suggests that as much as ~ 35 ^{7}Be nuclei cm^{-2} could have been dispersed in the atmosphere. We assume that these nuclei were deposited at altitudes above 150 km and that they adopted the density profile of the standard atmosphere at solar maximum. If all these conditions are true, then we estimate a ^{7}Be density of $\sim 10^{-7}$ atoms cm^{-3} at 310 km. Surprisingly, this is comparable to the density implied by the *LDEF* measurement. More detailed calculations are necessary to determine whether this is a realistic suggestion. We also note that some fraction of the ^{7}Be might also have been produced by spallation in the lower atmosphere from the intense flux of solar protons reaching Earth during this highly active period (J. Adams 1996, private communication). If the high atmospheric concentration of ^{7}Be found in *LDEF* originated in solar flares as we suggest, we would expect much lower concentrations to be found in recent satellite collections made near solar minimum that are currently being analyzed (G. W. Phillips 1996, private communication; B. Phlips 1997, private communication).

In a recent paper, Kotov et al. (1996) suggest that "nonthermal processes in the atmospheres of stars can play an important role in the production of the light elements, ^{7}Li in particular." This conclusion is based on *Yohkoh* observations of what they interpret to be the α-α fusion lines in two solar flares. As we mentioned above, the intensities in these lines were at least an order of magnitude higher than the mean observed by *SMM* relative to the well-studied carbon de-excitation line at 4.43 MeV. A puzzling aspect of the spectra displayed by Kotov et al. (1996) is the lack of any evidence of the 0.511 keV annihilation line that is so prevalent in the *SMM* spectra. Our studies indicate that the annihilation line is at least an order of magnitude more intense than the ^{7}Li line. This suggests to us that the 0.511 keV line in *Yohkoh* may have been misidentified as the α-α line complex.

Our conclusions concerning the accelerated α/proton ratio would not have been possible without access to a code developed jointly by Reuven Ramaty, Benzion Kozlovsky, Richard Lingenfelter, and one of us (R. J. M). We wish to thank them for giving us permission to use their code for this purpose. We also wish to thank them and Don Reames for their suggestions concerning this work. This work was supported by NASA DPR W-18995.

REFERENCES

Fishman, G. J., et al. 1991, Nature, 349, 678
Gabriel, A. H., et al. 1995, Adv. Space Res., 15 (7), 63
Gloeckler, G., & Geiss, J. 1989, in AIP Conf. Proc. 183, Cosmic Abundances of Matter, ed. C. J. Waddington (New York: AIP), 49
Grevesse, N., Noels, A., & Sauval, A. J. 1996, in ASP Conf. Ser. 99, Cosmic Abundances, ed. S. Holt & G. Sonneborn (San Francisco: ASP), 117
Hua, X.-M., & Lingenfelter, R. E. 1987, ApJ, 323, 779
Kotov, Yu. D., Bogovalov, S. V., Endalova, O. V., & Yoshimori, M. 1996, ApJ, 473, 514
Kozlovsky, B., & Ramaty, R. 1974, ApJ, 191, l43
———. 1977, ApJ, 19, L19
Laming, J. M., & Feldman, U. 1994, ApJ, 426, 414
Miller, J. A., & Reames, D. V. 1996, in AIP Conf. Proc. 374, High-Energy Solar Physics, ed. R. Ramaty, N. Mandzhavidze, & X.-M. Hua (New York: AIP), 450
Murphy, R. J., et al. 1997, ApJ, submitted
Murphy, R. J., Hua, X.-M., Kozlovsky, B., & Ramaty, R. 1990, ApJ, 351, 299
Murphy, R. J., Kozlovsky, B., & Ramaty, R. 1988, ApJ, 331, 1029
Murphy, R. J., Ramaty, R., Kozlovsky, B., & Reames, D. V. 1991, ApJ, 371, 793
Phillips, G. W., et al. 1991, Adv. Astron. Sci., 74, 575
Ramaty, R., Mandzhavidze, N., & Kozlovsky, B. 1996, in AIP Conf. Proc. 374, High-Energy Solar Physics, ed. R. Ramaty, N. Mandzhavidze, & X.-M. Hua (New York: AIP), 172
Ramaty, R., Murphy, R. J., & Dermer, C. D. 1987, ApJ, 316, L41
Reames, D. V. 1995, Adv. Space Res., 15 (7), 41
Reames, D. V., Cane, H. V., & von Rosenvinge, T. T. 1990, ApJ, 357, 259
Reames, D. V., Meyer, J. P., & von Rosenvinge, T. T. 1994, ApJS, 90, 649
Share, G. H., Harris, M. J., Leising, M. D., & Messina, D. C. 1993, A&A, 97, 341
Share, G. H., & Murphy R. J. 1995, ApJ, 452, 933
Van Hollebeke, M. A. I., McDonald, F. B., & Meyer, J. P. 1990, ApJS, 73, 285
Yoshimori, M., Suga, K., Morimoto, K., Hiraoka, T., Sato, J., Kawabata, K., & Ohki, K. 1994, ApJS, 90, 639